

A Study of leakage in Partial Wave Analysis  
for the  
HALL D Detector at Jefferson Lab

Ben Zaroukian and Jeffrey Kaditz

December 7, 2001

**Abstract**

The partial wave analysis of the reactions  $\gamma p \rightarrow \pi\pi\pi N$  for two different final states have been used to detector design issues related to resolution, low energy thresholds and particle reconstruction. These studies indicate that the resolution of the Barrell Calorimeter is one of the most sensitive parameters to minimizing feedthrough into the exotic  $1^{-+}$  channel.

# 1 Introduction

The Thomas Jefferson National Accelerator Facility (JLAB) in Newport News, VA is a new facility that is utilizing high energy electron and photon beams to study the structure of nuclear matter. JLAB is currently planning to double the energy of its accelerator with the main physics emphasis on experiments to try and explain why the constituents which build the protons and neutrons (quarks) are forever confined inside their parent particle. This particular question has been listed in the New York Times as one of the most important scientific questions of the new millennium. To attack this problem, an international group of physicists has come together to build a entirely new beam line and detector at the lab, known as Hall D. Carnegie Mellon is currently one of the leading institutions on this \$35,000,000 detector. The current plan is to be able to start taking data with this detector in early '2007.

One of the signatures of this physics is a new type of subatomic particle that has so called *exotic quantum numbers*. In order to identify when these new particles have been created, and to measure their quantum numbers, one performs a type of analysis called a *Partial Wave Analysis*. For this sort of analysis to work, it is necessary that the experiment be designed with it specifically in mind. As such, it is extremely important to optimize the detector for such an analysis.

In order to optimize the Hall D detector for the physics goals, it needs to be optimized in performing a partial wave analysis. The goal of this research project was to study detector systematics and to optimize the detector's design. This was performed by systematically varying a large number of detector parameters and observing what consequence this had on the detectors ability to carry out a good Partial Wave Analysis. Our results show, most noticeably, that even slight imperfections in the detector, can cause a strong signal in the  $a_1(1270)$  S-wave decay to feed into the corresponding D-wave decay. However, at least with the cocktail of states used in this analysis, it was quite difficult to get feed-through into the exotic, ( $J^{PC} = 1^{-+}$  channel).

## 1.1 Monte Carlo Events

In this study the GENR8 program was used to produce a sample of final state events. Approximately 9 million events of the following two types were generated.

$$\gamma p \rightarrow X^+ n \rightarrow \pi^+ \pi^+ \pi^- n \quad (1)$$

$$\gamma p \rightarrow Y^+ n \rightarrow \pi^+ \pi^0 \pi^0 n \rightarrow \pi^+ \gamma \gamma \gamma n \quad (2)$$

These events were then weighted with a physics hypothesis based on a one-pion exchange model in which the resonances  $X$  and  $Y$  would decay via a

$\rho\pi$  state to the  $3\pi$  final state. The physics assumed that the  $a_1(1260)$ , the  $a_2(1320)$  and the  $\pi_2(1670)$  were produced. The  $a_1$  was then allowed to decay into  $\rho\pi$  in both an S- and a D-wave. The  $\pi_2$  was allowed to decay to  $\rho\pi$  in both a P- and an F-wave. The resulting events were then run through the Hall D detector Monte Carlo, `HDFAST`. Approximately 200,000 events survived in each of the two reaction channels.

Reaction 1 involved the detection and reconstruction of only charged pions. This was used to test detector components designed to detect charged particles. The changes tested with this reaction are:

1. The Magnetic Field:

A mismatch was made between the magnetic field with which the physics events were tracked, and between what was used in the normalization integral. While this exact change is unlikely to affect the detector, it is easy to make to the geometry and produced a good starting point to the entire study. Its effect is to produce a global smearing of tracking parameters.

2. The Forward Drift Chamber Resolution:

Earlier resolution studies indicated that the resolution of the the forward drift chamber system was an important parameter. It is clear that this system is responsible for detecting fast forward particles, and the best momentum resolution is achieved with the best resolution in the forward chambers.

3. The Forward Drift Chamber Beam Hole Size:

In this study a mismatch was created between the size of the beamline hole in forward chambers between the physics events samples, and the normalization events. This attempts to simulate a problem in understanding the efficiency in the very forward directions.

Reaction `/refeq:neutral` focused on the detection of the  $4\gamma$ 's coming from the two  $\pi^0$  decays. This reaction was used to test the detector components specifically designed to detect photons, namely the Barrel Calorimeter and the Lead Glass Detector. The changes tested with this reaction are listed below.

1. The low energy threshold of the Barrel Calorimeter.

Here we varied the minimum photon energy that could be reconstructed in the Barrel Calorimeter. The nominal design value is  $20\text{ MeV}$ .

2. The low energy threshold of the Lead Glass Detector.

Here we varied the minimum photon energy that could be detected in the Pb-Glass system. The nominal value is  $100\text{ MeV}$ .

3. Resolution Parameters for the Barrel calorimeter.

Two parameters control the resolution of the Barrel Calorimeter. A constant offset and a percentage resolution parameter. Here we varied both of these for the Barrel Calorimeter.

4. Resolution Parameters for the Lead Glass Detector.

A similar set of parameters control the behavior of the Lead-Glass detector. These parameters have been varied here.

Both reactions were simulated using a photon beam energy of  $8.5\text{ GeV}$ . Each event was run through the HDFast detector simulation with the varied geometry parameters, and then PWA was performed on the resulting data. The data used to normalize the PWA was also run through the same detector simulation. The physics channels simulated in the data are given above. The goal of this study was to see the signal strength in a channel that was not put in the original cocktail, leakage. The following set of partial waves are physically possible to photoproduce in  $\gamma p$  reactions.

1. A  $\pi_1$  particle,  $J^{PC} = 1^{-+}$ . This is the very inetersting wave as it has exotic, or non- $q-\bar{q}$  quantum numbers.
2. An  $a_3$  particle,  $J^{PC} = 3^{++}$ , which would be produced in either the  $+$  or  $-1$  magnetic substate.

In addition to the above two, it is not possible to physically produce an  $a_2$  in either the  $+$  or  $-2$  magnetic substates, but we could have leakage into this state. Finally, a critical source of leakage would be to look at one of the produced signals which is quite strong leaking into one of the weaker channels. The two examples of this in this data set are the  $a_1$  decaying via S-wave leaking into the D-wave decay, and the  $\pi_2$  decaying via P-wave leaking into the F-wave.

## 2 Results

### 2.1 PWA results for $\pi^+\pi^+\pi^-$ reaction

The nominal results for reaction 1,  $(\pi^+\pi^+\pi^-)$  are shown in Figures 1 and 2. There is virtually no leakage into the any of the nonexistent channels as seen in 2.

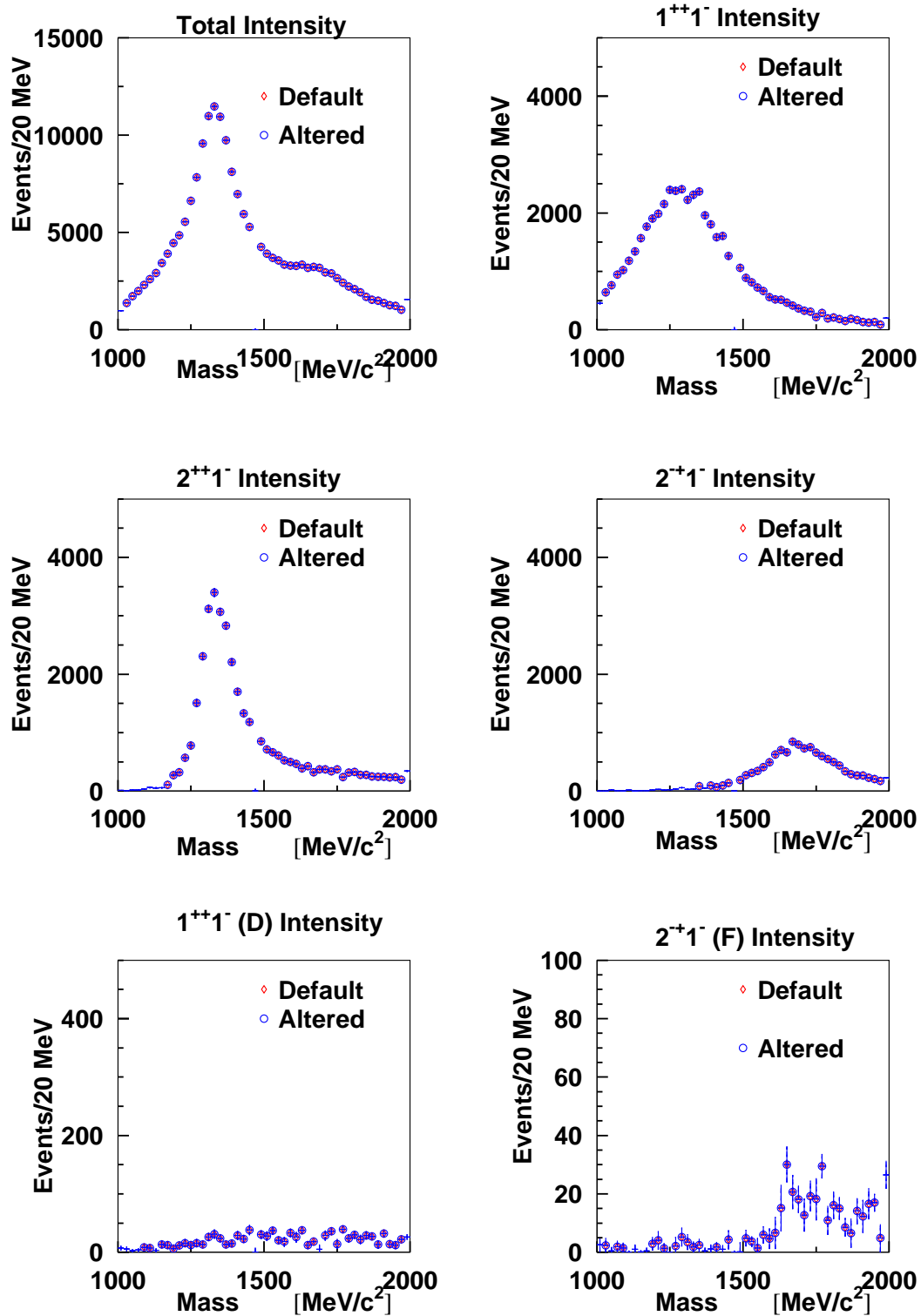


Figure 1: PWA results for reaction 1 using the default geometry specifications. These results show the intensity for everything, and then the three major components,  $a_1$  decaying via S-wave, or  $1^{++}$ ,  $a_2$  or  $2^{++}$  and the  $\pi_2$  decaying via P-wave, or  $2^{-+}$ . The bottom two figures show the weaker  $a_1$  D-wave and the  $\pi_2$  F-wave results.

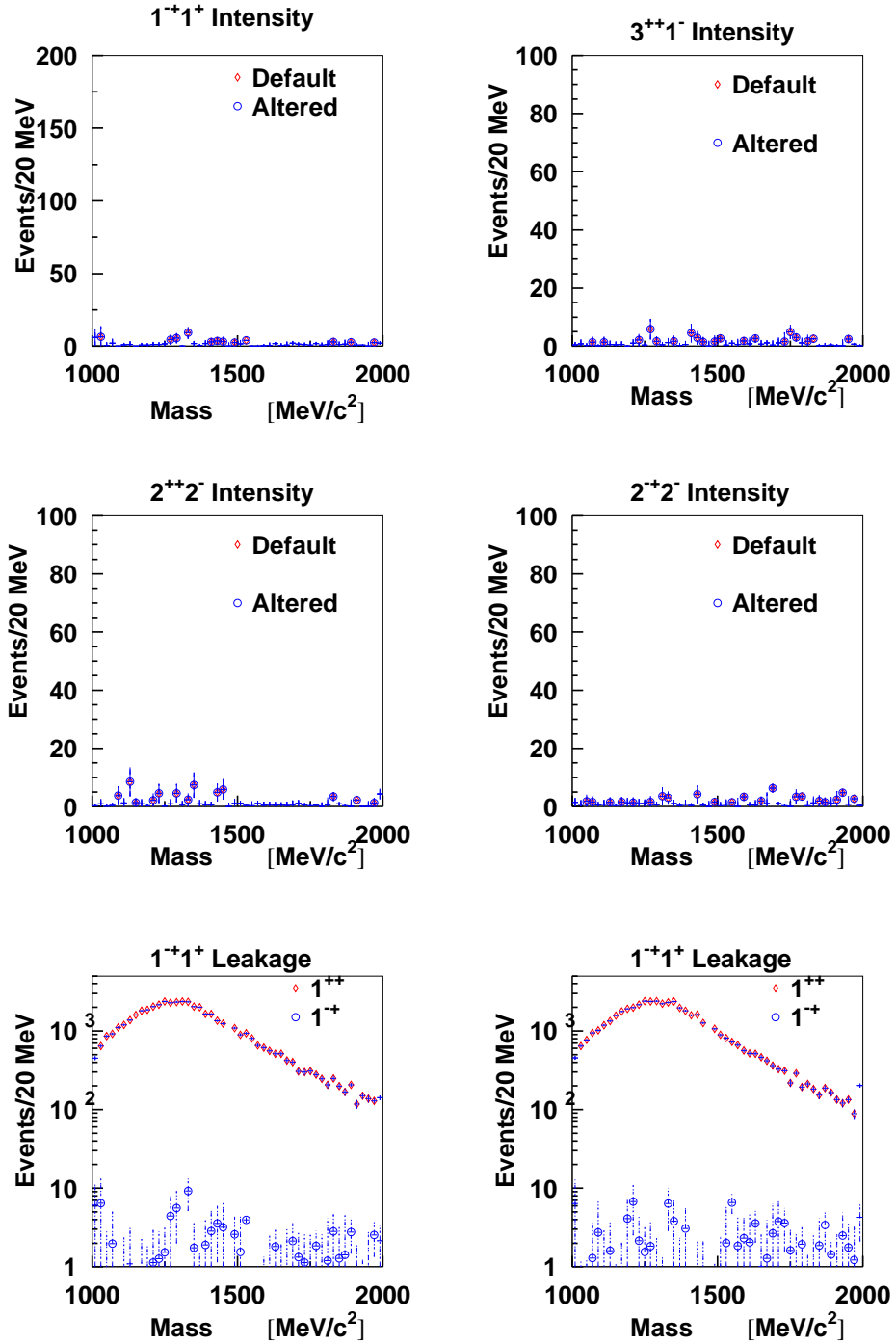


Figure 2: PWA results for reaction 1 using the default geometry specifications. These results show the intensity for the waves that are not physically present in the data set. The  $1^-+$  wave is the exotic  $\pi_1$  channel. The bottom two figures show the strength of the leakage into the exotic  $1^-+$  wave compared to the strength of the  $1^-+$  signal — the latter is believed to be the source of the leakage. The level of the leakage is below 1% for the nominal detector configuration.

## 2.2 Smearred Results for Reaction 1

A series of smearings were used to probe the effects on the partial wave analysis.

### 2.2.1 Magnetic Field Smearing

Initially, the magnetic field map used to track the physics events was distorted with respect to that used in the normalizations. Table 1 shows the various field values tested under this scenario. For the most part, these variations had little effect on the PWA results. Figure 3 shows the feed-through into the exotic channel for the case of  $-10\%$  and  $+20\%$  changes to the magnetic fields. These are fairly extreme changes to the field strength, and not typical of what would be expected under normal running conditions. These results indicate that globally, the charged tracking system is good.

-20%	-10%	-4%	-2%	-1%	+0%	+1%	+10%	+20%
------	------	-----	-----	-----	-----	-----	------	------

Table 1: Magnetic field values used in the charge testing. The nominal field value is  $2.24 T$ .

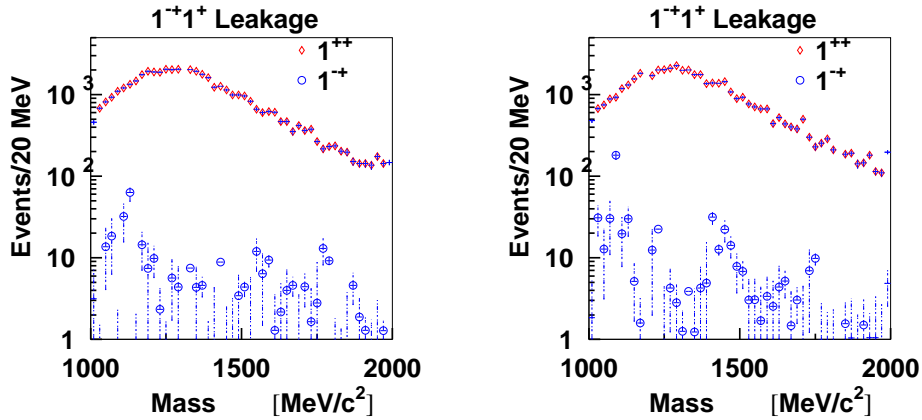


Figure 3: Feed-through into the exotic  $1^{-+}$  wave when the field values have been distorted by  $-10\%$  (left) and  $+20\%$  (right). The signal is compared to the strength of the  $1^{++}$  channel which is believed to be the origin of this feed-through. The intensity of the feed-through is about  $1\%$  of the  $a_1$  signal.

### 2.2.2 Hole size in the forward direction

A typical acceptance problem in partial wave analysis is that the exact boundaries of a hole are not well understood. In order to study this, we varied the

size of the hole around the beamline in the forward detectors. The nominal hole along the beamline is  $3.5\text{ cm}$  radius. In performing these studies, the hole size in the normalization integral was left alone, but that in the physics events was varied. The range of hole sizes are shown in Table 2, while the leakage into the exotic waves are shown in Figure 4. As can be seen, the leakage into the exotic wave is very small, even for extreme changes. Actually, the reason for this is that to produce an exotic wave, we need to break a forward-backward or up-down symmetry in the detector. This sort of change will produce no such asymmetry. However, this sort of change can distort an *even* distribution to look like a *higher order* even distribution. For example, it would be possible to produce leakage from a strong S-wave into a weaker D-wave. Such an effect can be seen in

3.0 cm	3.75 cm	4 cm	5 cm	10 cm
--------	---------	------	------	-------

Table 2: Hole size in the forward direction used in simulating the physics events.

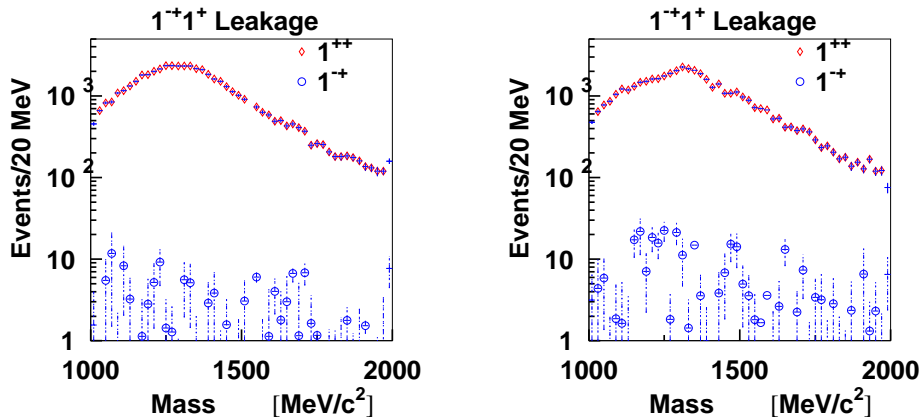


Figure 4: These plots show the exotic  $1^{-+}1^{-}$  wave for changes in the forward hole geometry. The left plot is with the central hole radius of the FDC at  $3\text{ cm}$  (default is  $3.5\text{ cm}$ ). The right picture is with the whole size set to  $10\text{ cm}$ . Both signals are compared to the  $1^{++}$  signal, which is believed to be the source of the leakage. Neither of these changes produces significant leakage above 1% into the exotic wave.

### 2.2.3 Resolution of the Forward Chambers

The nominal resolution of the forward drift chamber systems is  $150\ \mu\text{m}$ . We have also run a comparison with this resolution degraded to  $300\ \mu\text{m}$  in reconstructing the physics events, but left at the nominal value for the normalization events. The results of this are shown in Figure 5



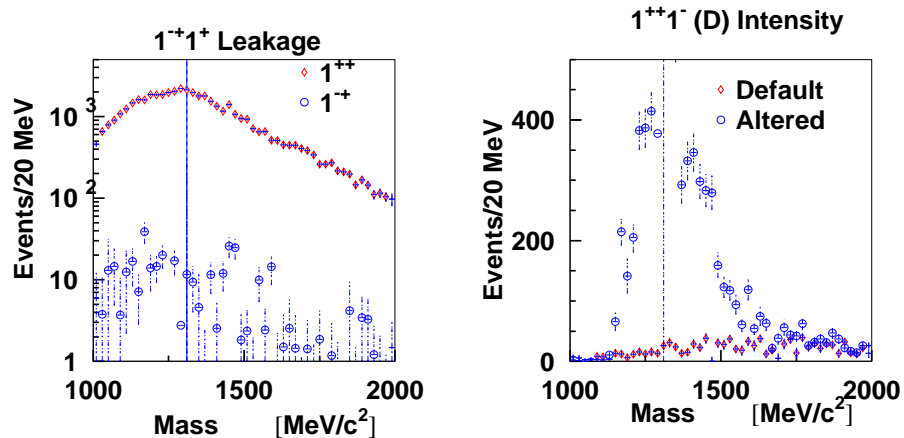


Figure 5: The left hand plot shows the leakage into the exotic  $1^{-+}$  wave compared to the  $1^{++}$  wave. The right hand figure shows the leakage into the  $1^{++}$  D-wave that comes from the  $1^{++}$  S-wave. Typical leakage into the exotic wave of about 1% is observed, while a large leakage into the D-wave is seen.

### 2.3 PWA results for $\pi^+\pi^0\pi^0$ final state.

Reaction 2,  $\pi^+\pi^0\pi^0$  was simulated for the primary purpose of testing the neutral particle detectors. The barrel calorimeter and the lead glass detector. Both of these detectors have a minimum detectable photon energy, which in the standard Monte Carlo is  $20\text{ MeV}$  for the Barrel Calorimeter and  $100\text{ MeV}$  for the Lead Glass detector. In addition, there is a two parameter photon energy resolution that can be varied for each detector. The results for standard geometry are shown in Figures 6 and 7.

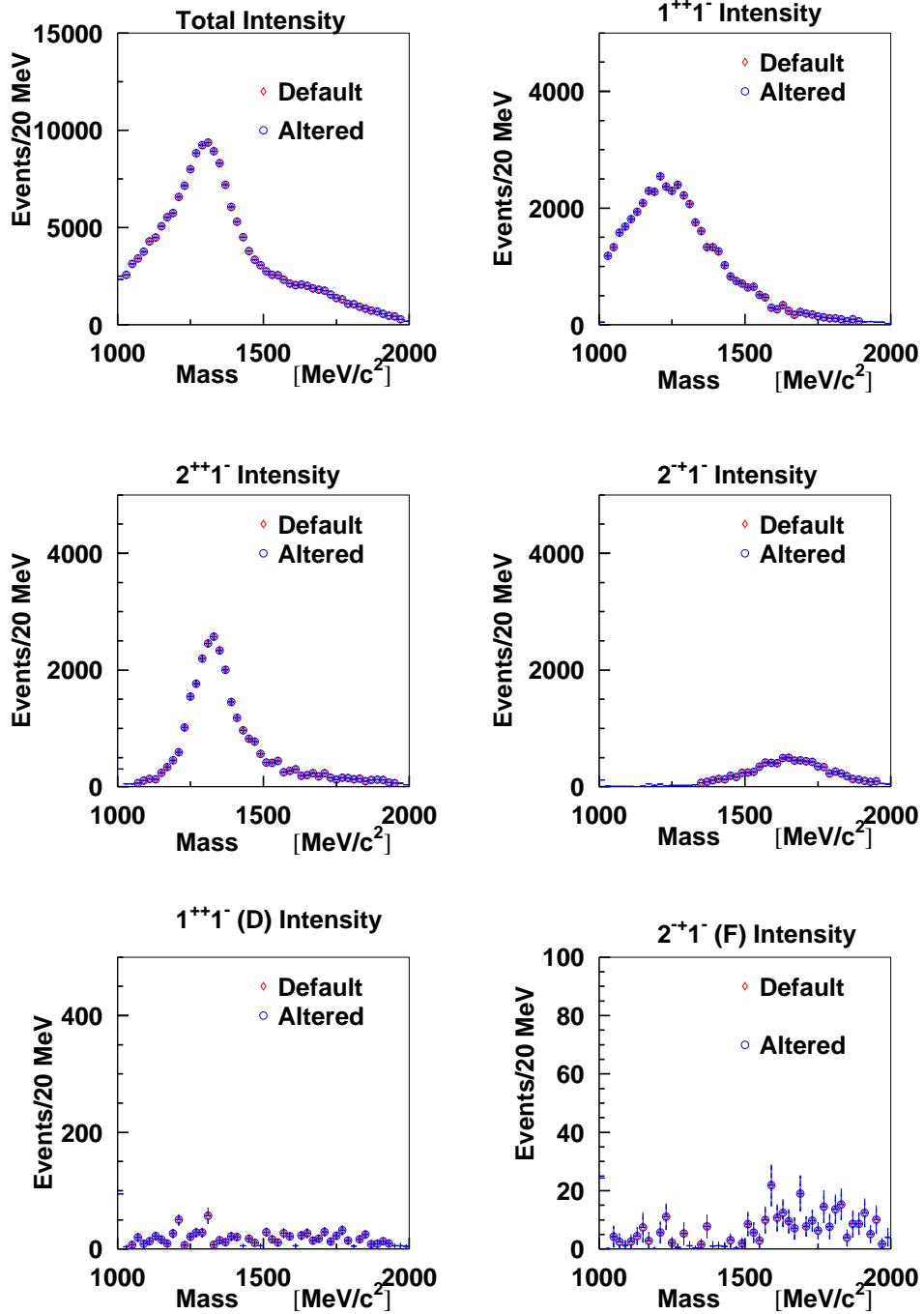


Figure 6: These PWA plots are for reaction 2 ( $\pi^+\pi^0\pi^0$ ) with default geometry specifications.

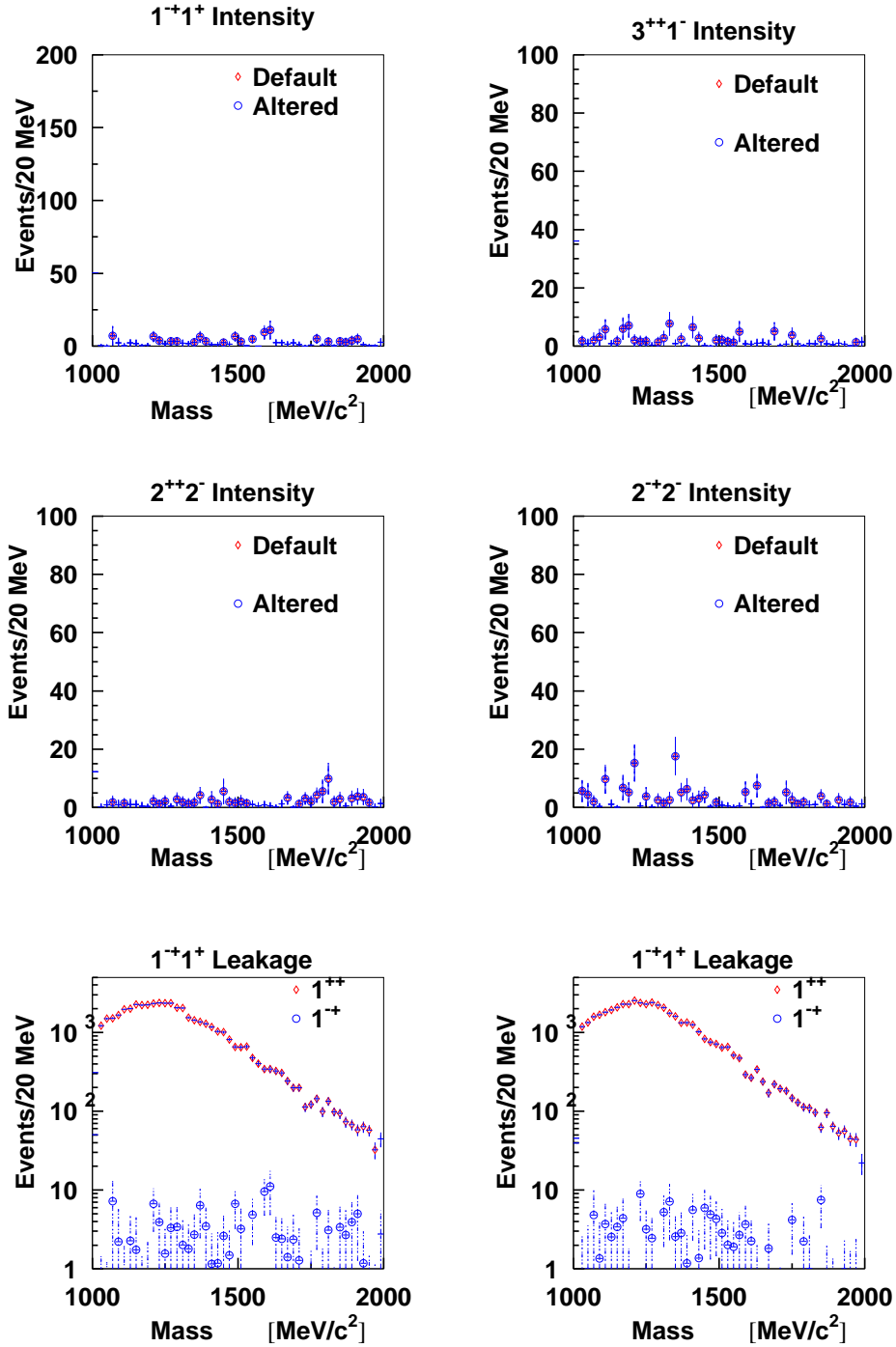


Figure 7: PWA results for reaction 2 using the default geometry specifications. These results show the intensity for the waves that are not physically present in the data set. The  $1^{-+}$  wave is the exotic  $\pi_1$  channel. The bottom two figures show the strength of the leakage into the exotic channel compared to the  $1^{++}$  channel.

### 2.3.1 Low energy photon cutoffs in the Barrel Calorimeter

$E_\gamma \geq 20 \text{ MeV}$	$E_\gamma \geq 35 \text{ MeV}$	$E_\gamma \geq 50 \text{ MeV}$
--------------------------------	--------------------------------	--------------------------------

Table 3: The design value for the detector is  $20 \text{ MeV}$ . Results were also run using  $35 \text{ MeV}$  and  $50 \text{ MeV}$  as the low energy cutoff for physics events as seen in the barrel calorimeter.

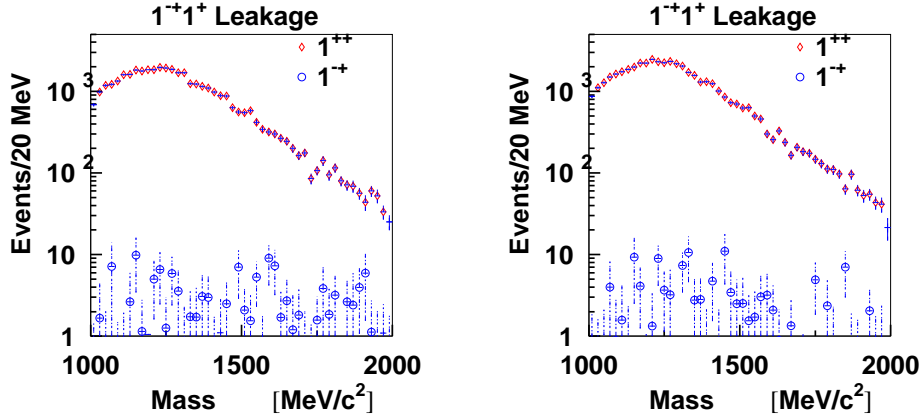


Figure 8: These plots show the leakage in to the exotic  $1^-+1^-$  wave for a minimum detectable photon energy of  $35 \text{ MeV}$  and  $50 \text{ MeV}$  in the barrel calorimeter. The leakage is compared to the strength of the  $1^{++}$  signal, which is expected to be its source.

### 2.3.2 Low energy photon cutoffs in the Lead Glass Detector

$E_\gamma \geq 100 \text{ MeV}$	$E_\gamma \geq 150 \text{ MeV}$	$E_\gamma \geq 200 \text{ MeV}$
---------------------------------	---------------------------------	---------------------------------

Table 4: The design value for the detector is  $100 \text{ MeV}$ . Results were also run using  $150 \text{ MeV}$  and  $200 \text{ MeV}$  as the low energy cutoff for physics events as seen in the barrel calorimeter.

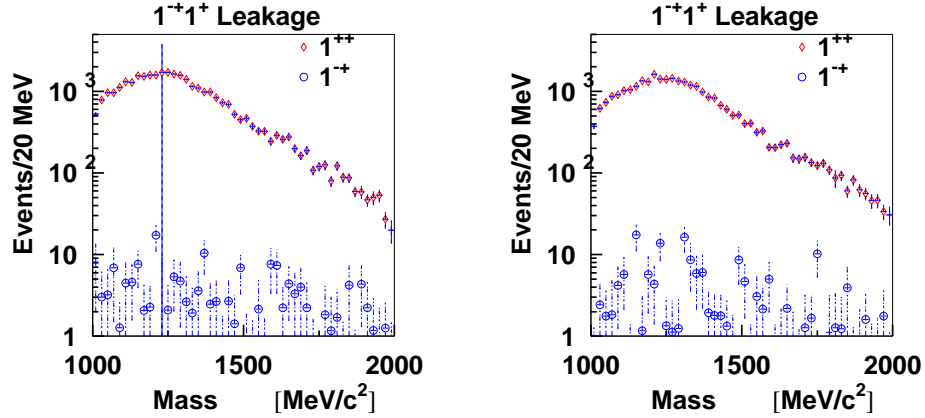


Figure 9: These plots show the leakage in to the exotic  $1^{-+}1^{-}$  wave for a minimum detectable photon energy of  $150 \text{ MeV}$  and  $200 \text{ MeV}$  in the Lead Glass calorimeter. The leakage is compared to the strength of the  $1^{++}$  signal, which is expected to be its source.

### 2.3.3 Barrel Calorimeter Resolution Changes

The parametrization of the barrel calorimeter showers are controlled by two parameters as given in the following formula:

$$\frac{\sigma_E}{E} = \frac{\sigma_a}{\sqrt{E}} + \sigma_b,$$

where the energy is expressed in units of  $GeV$ . The default values for the two parameters are:  $\sigma_a = 0.06$  and  $\sigma_b = 0.01$ . During these studies, we examined the following combinations as given in Table 5. In looking at the results in Figure 10, it at first appears that the increase in  $\sigma_b$  as shown in the middle figures leads to a clear feed through at the few percent level. However, the plots for an even larger value of  $\sigma_b$  do not appear to confirm this effect. As such, it is difficult to conclude that this is going to be a problem.

$\sigma_a$	0.06	0.06	0.06	0.04	0.08
$\sigma_b$	0.01	0.02	0.03	0.01	0.01

Table 5: Tested resolution combinations for the the Barrel Calorimeter.

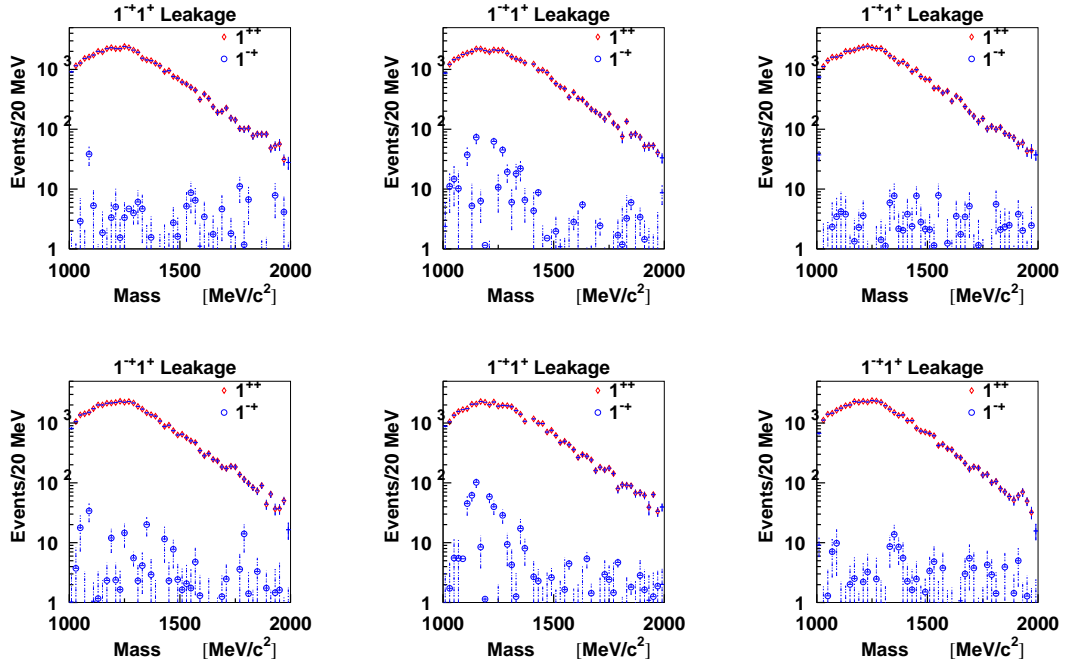


Figure 10: Changes to the Barrel Calorimeter resolution parametrization. The left hand picture has  $\sigma_a = 0.08$  and  $\sigma_b = 0.01$ , the middle picture has  $\sigma_a = 0.06$  and  $\sigma_b = 0.02$ , finally the right hand picture has  $\sigma_a = 0.06$  and  $\sigma_b = 0.03$ .

### 2.3.4 Lead Glass Calorimeter Resolution Changes

The parametrization of the lead glass calorimeter showers are controlled by two parameters as given in the following formula:

$$\frac{\sigma_E}{E} = \frac{\sigma_a}{\sqrt{E}} + \sigma_b,$$

where the energy is expressed in units of  $GeV$ . The default values for the two parameters are:  $\sigma_a = 0.06$  and  $\sigma_b = 0.01$ . During these studies, we examined the following combinations as given in Table 6.

$\sigma_a$	0.06	0.07	0.06	0.04	0.08
$\sigma_b$	0.01	0.01	0.03	0.01	0.01

Table 6: Tested resolution combinations for the the Barrel Calorimeter.

## 3 Conclusions

The most important conclusions of this report is that it is difficult to produce feed through into the exotic channel from other meson channels. For almost all changes made here, the amount of feed through was less than 1% of a strong channel, with the feed through for the nominal design values being something like 0.1%.

However, we do see significant leakage from the  $a_1$  S-wave decay into the  $a_1$  D-wave decay, with even small changes in the nominal detector design. This sort of feed through is fairly straight forward to understand. An S-wave decay is nominally flat, however, if we have losses near  $\cos\theta = \pm 1$ , the easiest description of this is with a D-wave component. In order to produce a P-wave component, it is necessary to produce a forward-backward asymmetry in the Jackson frame – something that appears fairly difficult to do with this detector.